ACCOUNTS
of chemical research

pubs.acs.org/accounts
Article

Unique Properties and Emerging Applications of Carbolong Metallaaromatics

Ming Luo, Dafa Chen, Qian Li, and Haiping Xia*

Cite This: https://doi.org/10.1021/acs.accounts.2c00750

Read Online

ACCESS | Metrics & More | Article Recommendations

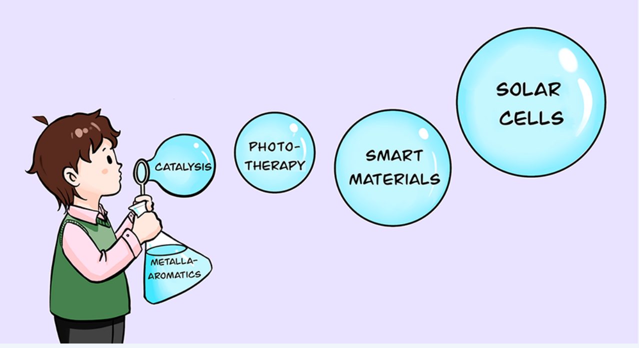

CONSPECTUS: Aromatic compounds are important in synthetic chemistry, biomedicines, and materials science. As a special type of aromatic complex, transition-metal-based metallaaromatics contain at least one transition metal in an aromatic framework. The chemistry of metallaaromatics has seen much progress in computational studies and synthetic methods, but their properties and applications are still emerging. In recent years, we have disclosed a series of metal-centered conjugated polycyclic metallacycles in which a carbon chain is chelated to a metal center through at least three metal−carbon bonds. These are termed carbolong complexes and exhibit good stability to water, oxygen, light, and heat on account of their polydentate chelation and aromaticity, making them easy to handle. Carbolong complexes are not only special π-conjugated aromatics but also organometallics; therefore, they have the properties of both species. In this Account, we showcase the recent advances in their applications based on their different properties.

First, carbolong complexes are a special kind of π-conjugated aromatic, with the ability to transmit electrons, allowing them to function as single-molecule conductors and candidates for electron transporting layer materials (ETLs) in solar cells. A series of carbolong complexes have been proved to be useful as achievable ETLs which enhance device performance in both organic solar cells and perovskite solar cells.

Second, due to the involvement of d orbitals in the conjugation, carbolong complexes normally exhibit strong and broad absorption, even in some cases extending to the near-infrared region (NIR). The absorbed optical energy can be converted into light, heat, and ultrasound; consequently, carbolong compounds can be used as core moieties in smart materials. For example, 7C carbolong complexes were found to exhibit aggregation-enhanced near-infrared emission (AIEE). Some 12C carbolong complexes have been designed into the core moieties of NIR-responsive polymers, such as cylindrical NIR-responsive materials, self-healing materials, and shape memory materials. In contrast to the stereotypically toxic osmium compounds such as the highly toxic OsO_4, some osmium carbolong complexes exhibit low cell cytotoxicity and good biocompatibility; consequently, they also have potential applications in the biomedical area. For example, benefiting from broad absorption in the NIR, 9C and 12C carbolong complexes have been used in photoacoustic imaging and photothermal therapy, respectively. In addition, photodynamic therapeutic applications which take advantage of a carbolong peroxo complex are discussed.

Third, as special transition-metal complexes chelated by carbon-based ligands, a carbolong peroxo complex has displayed catalytic activity in the dehydrogenation of alcohols and a bimetallic carbolong complex has been used to catalyze difunctionalization reactions of unactivated alkenes.

Overall, aromatic carbolong complexes have been applied to photovoltaics, smart materials, phototherapy, and catalytic reactions. Moving forward, we hope that this Account will shed light on future studies and theoretical research and encourage more discoveries of the properties of other metallaaromatics.

KEY REFERENCES

- Liu, L.; Chen, S.; Qu, Y.; Gao, X.; Han, L.; Lin, Z.; Yang, L.; Wang, W.; Zheng, N.; Liang, Y.; Tan, Y.; Xia, H.; He, F. Nanographene-Osmapentalyne Complexes as a Cathode Interlayer in Organic Solar Cells Enhance Efficiency over 18%. *Adv. Mater.* **2021**, 33, 2101279.[1] *This article reveals the expansion of the π conjugation by*

Received: November 5, 2022

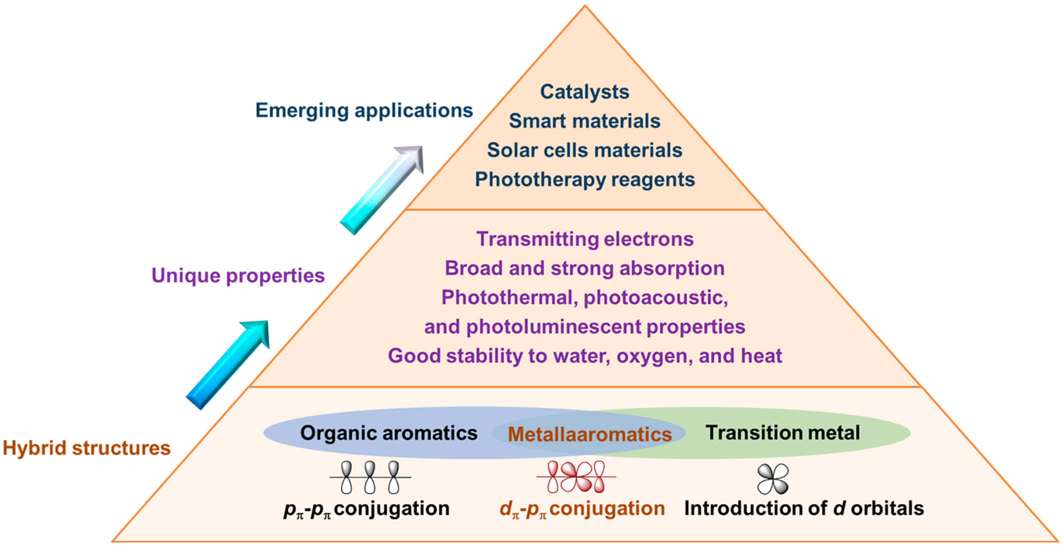

Figure 1. Research pyramid for metallaaromatics.

covalently bonding HBC with two 7C carbolong complexes, achieving the highest PCE with an extension of π conjugation.

- Chen, Y.; Yang, L.; Zheng, W.; Ouyang, P.; Zhang, H.; Ruan, Y.; Weng, W.; He, X.; Xia, H. Dynamic Polymer Network System Mediated by Radically Exchangeable Covalent Bond and Carbolong Complex *ACS Macro Lett.* **2020**, *9*, 344−349.[2] *This communication describes how metallaaromatics were designed into the core moieties of NIR self-healing polymers.*
- Zhu, C.; Yang, C.; Wang, Y.; Lin, G.; Yang, Y.; Wang, X.; Zhu, J.; Chen, X.; Lu, X.; Liu, G.; Xia, H. CCCCC Pentadentate Chelates with Planar Möbius Aromaticity and Unique Properties. *Sci. Adv.* **2016**, *2*, e1601031.[3] *This article reports the photothermal therapy of metallaaromatics in vivo for the first time.*
- Cui, F.-H.; Hua, Y.; Lin, Y.-M.; Fei, J.; Gao, L.-H.; Zhao, X.; Xia, H. Selective Difunctionalization of Unactivated Aliphatic Alkenes Enabled by a Metal-Metallaaromatic Catalytic System. *J. Am. Chem. Soc.* **2022**, *144*, 2301−2310.[4] *This article highlights metal−metallaaromatics cooperative catalysis for the difunctionalization of unactivated alkenes.*

1. INTRODUCTION

Organic aromatics are conjugated cyclic compounds with delocalized π electrons, which represent one of the most fundamentally important families in chemistry. Aromatic compounds have been broadly studied and applied in theoretical research,[5] synthetic chemistry,[6] materials science,[7] and biomedicines;[8] consequently, they play a significant role in daily life and development in society.

Metallaaromatics can be viewed as organic aromatic compounds which incorporate at least one transition metal in the aromatic frameworks. Forty years ago, Roper et al. crystallographically characterized the first metallabenzene[9] following theoretical predictions by Thorn and Hoffmann.[10] Subsequently, the chemistry of metallaaromatics has experienced enormous growth and development.[11−13] To date, various metallaaromatics including metallabenzenes,[14] metallabenzynes,[15] dianion metalloles,[16] spiro metalloles,[17] heterometallaaromatics,[18] metallapentalenes,[19] and metallapentalynes[20] have been successfully prepared.

Structural novelty leads to special physical and chemical properties and may generate new applications. Metallaaromatics are hybrid structures of organic aromatics and transition-metal complexes through d_π−p_π conjugation and consequently own unique properties of both kinds. For example, they can transmit electrons and exhibit broad and strong absorption thanks to d_π−p_π conjugation, and as a result, they are employed as the ETLs in solar cells and NIR materials in smart materials and phototherapy reagents. They also can be viewed as carbon-based transition-metal complexes with cyclic carbenes which are utilized in homogeneous catalysis (Figure 1).

In recent years, we have developed a series of properties and applications of aromatic carbolong complexes (nC carbolong complexes mean n-atom unsaturated carbon chain chelates to a transition metal). For example, 7C carbolong complexes were found to exhibit AIEE;[20] 9C and 12C carbolong complexes have been used for photoacoustic imaging,[21,22] photothermal therapy,[3,22,23] and in photothermally responsive materials;[2,24−27] a carbolong peroxo complex has been utilized in photodynamic therapy[28] and the catalytic dehydrogenation of alcohols;[29] and a bimetallic carbolong complex has been used to catalyze the difunctionalization of alkenes (Scheme 1).[4] In this Account, we have highlighted and discussed recent research on the properties and applications of metallaaromatics

Scheme 1. Representative Carbolong Complexes Discussed in This Account

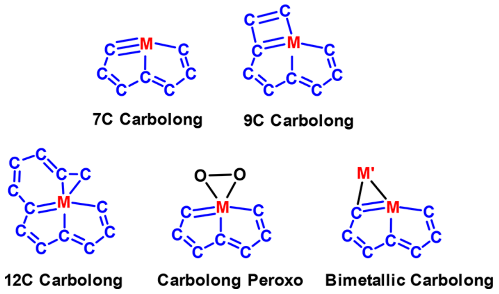

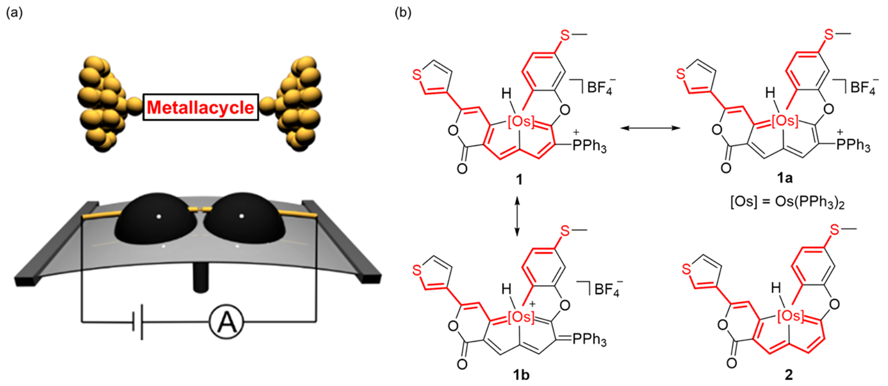

Figure 2. (a) Schematic of the MCBJ device. (b) Chemical structures of metallaaromatics **1** and **2**. (The red lines describe the charge-transport pathway.) Adapted with permission from ref 30. Copyright 2017 American Chemical Society.

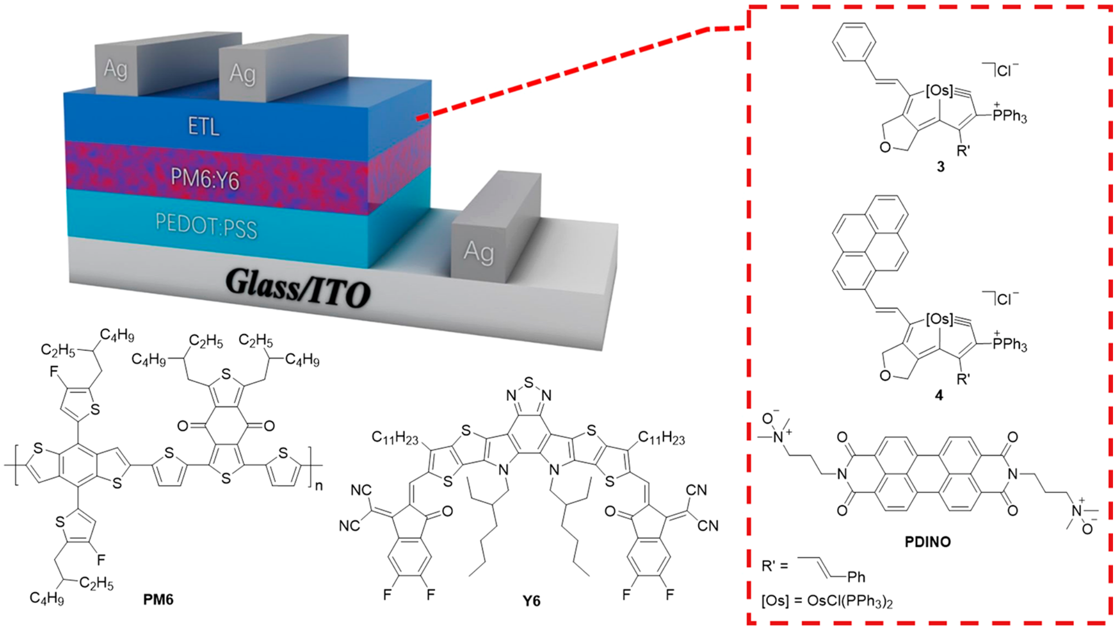

Figure 3. Applications in PM6:Y6-based OSCs. Reproduced with permission from ref 31. Copyright The Authors, some rights reserved; exclusive license Springer Nature. Distributed under a Creative Commons Attribution License 4.0 (CC BY) https://creativecommons.org/licenses/by/4.0/.

that were mainly developed by our group. We anticipate that our contributions will promote their further research.

2. APPLICATIONS IN SINGLE-MOLECULE CONDUCTORS AND SOLAR CELLS

Carbolong complexes can transmit electrons by behaving as special π-conjugated aromatics. They can be employed as single-molecule conductors and alternatives for electron-transporting layer materials (ETLs) or cathode interlayer materials (CILs) in solar cells.

2.1. Single-Molecule Conductors

The field of molecular electronics investigates the charge transport across the molecular building blocks linking nanogap electrodes in which most of the building blocks studied are traditional aromatic frameworks. In this regard, the charge-transport pathways of metallaaromatics **1** and **2** with anchoring groups were explored using a mechanically controllable break junction (MCBJ) (Figure 2a).[30] The phosphonium group increases the delocalization and improves the conductance of **1** by more than 1 order of magnitude in comparison to that of **2**, opening a new avenue to tuning the charge transport in molecular electronics (Figure 2b).

2.2. Applications in Solar Cells

Solar cells convert light directly into electricity through the photovoltaic effect. Two typical solar cells are organic solar cells (OSCs) and perovskite solar cells (PSCs). Prior studies have shown that carbolong complexes can transmit electrons, and it is thought that they could serve as one of the layer materials in solar cells and so enhance the cells' efficiency.

2.2.1. Applications in OSCs. Recently, we developed a facile approach to the construction of a $d_\pi - p_\pi$ conjugation system via a reaction of M$\equiv$C and C$\equiv$C bonds.[31] Inspired by π-conjugated molecules that have been employed in engineering interfaces of OSCs, we compared the performance of the unique $d_\pi - p_\pi$ conjugated systems as ETLs with that of common interfacial materials (PDINO) in PM6:Y6 based OSCs. To our surprise, the power conversion efficiencies (PCEs) of complexes **3** and **4** (15.76 and 16.28%, respectively) are higher than that of PDINO (15.06%) by improving carrier transport as a result of the extended π conjugation (Figure 3).

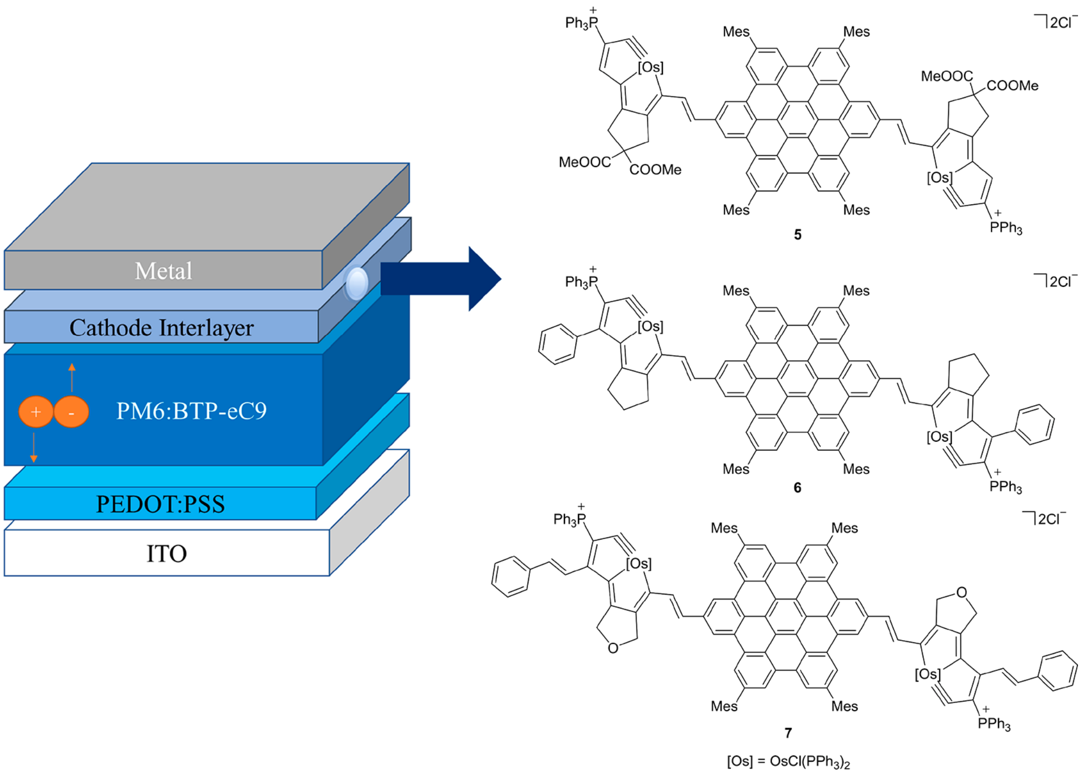

Figure 4. Structure of bulk heterojunction NFSC and chemical structures of CILs. Adapted with permission from ref 1. Copyright 2021 Wiley-VCH Verlag GmbH.

Inspired by the good performance of $d_\pi-p_\pi$ conjugated systems in OSCs, we sought to expand the π conjugation by covalently bonding nanographene hexabenzocoronenes (HBC) with 7C carbolong complexes (**5**, **6**, and **7**) which perform as CILs to enhance the ability of transmitting electrons.[1] The PCE of PM6:BTP-eC9-based nonfullerene solar cells (NFSC) exceeded 18% (Figure 4).

2.2.2. Applications in PSCs. In addition to applications in organic solar cells, a series of carbolong complexes were recently employed as CILs to improve the efficiency and stability of inverted PSCs.[32−34] For example, the PCEs of devices modified with irida-carbolong **8** and its derivative **9** were boosted by up to 20.02 and 21.29%, respectively (Figure 5).

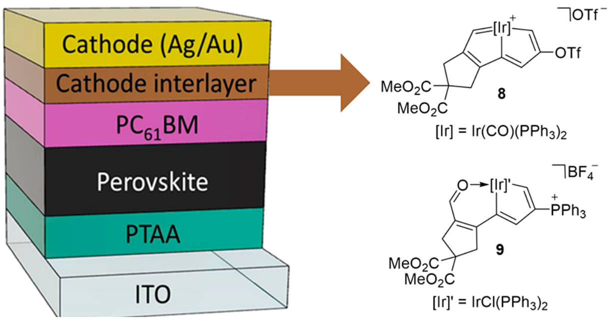

Figure 5. Structure of PSCs and chemical structure of CILs. Adapted with permission from ref 32. Copyright 2021 American Chemical Society.

3. PHOTOPHYSICAL PROPERTIES AND APPLICATIONS IN SMART MATERIALS AND PHOTOTHERAPY REAGENTS

Due to the action of d orbitals in the conjugated systems, carbolong complexes normally exhibit strong and broad absorption, sometimes even extended to the NIR. With the transformation of absorbed energy to light, they have photoluminescent properties. On the other hand, as the conversion of the absorbed optical energy into heat and ultrasound proceeds, they could be designed as core units in smart materials, photoacoustic imaging, and phototherapy reagents.

3.1. Photoluminescent Properties

In 2013, we synthesized osmapentalyne, the first carbolong complex[20] (Figure 6a). Interestingly, this osmapentalyne exhibits AIEE with large Stokes shifts and long lifetimes compared to that of traditional organic dyes. The excitation of **10** led to NIR emission due to integration of the osmium atom into the aromatic conjugation, which is comparable to those of luminescent lanthanide complexes with antenna ligands.[35] Adding excess water to the ethanol solutions of **10** led to the enhancement of the emission intensity because $\pi-\pi$ stacking is sterically precluded by the bulky PPh_3 ligands (Figure 6a). Consistent with the previous findings, red emission was observed from crystals of **10** (Figure 6b, inset). The emission lifetimes of **10** are in the range of $10^{-7}-10^{-6}$ s as a consequence of a partially forbidden luminescent electronic transition.

3.2. Applications in Smart Materials

Smart materials are designed to be controlled by external stimuli, such as light, temperature, and chemicals, and they possess many applications, including sensors, self-healing

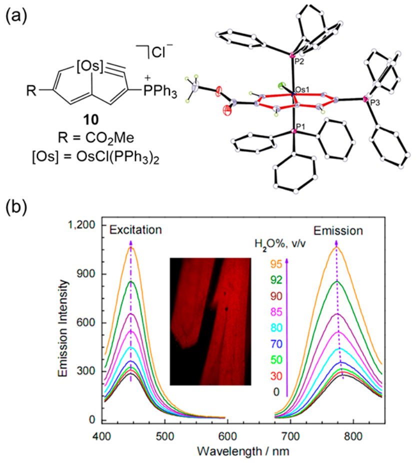

Figure 6. (a) Chemical structure and crystal structure of **10**. (b) Time-dependent emission decay of **10** in ethanol/water solutions (inset: fluorescent photomicrograph of the crystals). Adapted with permission from ref 20. Copyright 2013 Springer Nature.

materials, and shape memory materials.[36] Carbolong complexes exhibit good photothermal effects in NIR, and because of this, they have been designed for use as NIR photothermally responsive materials.

3.2.1. Applications in Photothermal Phase-Transition Materials.

An osmapentalenofuran with a terthiophene group displays a significant photothermal effect as the temperature is increased from 28 to 57 °C within 5 min under NIR irradiation.[37] Based on this observation, we synthesized a carbolong complex (**11**) containing a methacrylate group as a monomer. Then, this monomer was copolymerized with oligo(ethylene glycol) methacrylate to afford a new type of stimulus-responsive metal-containing polymer (**12**) (Figure 7a). Upon exposure to NIR (808 nm, 1.0 W cm^{-2}), the temperature of a solution of metallaaromatic polymer **12** rose quickly and the solutions became turbid, indicating the occurrence of a phase transition (Figure 7b,c).

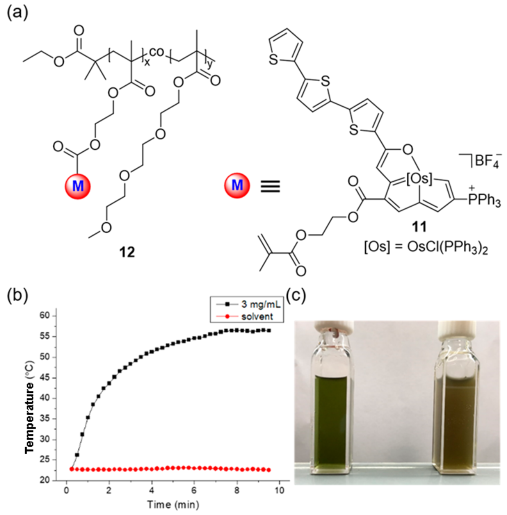

Figure 7. (a) Structure of a metallaaromatic polymer (**12**). (b) Photothermal effect of the metallaaromatic polymer (**12**). (c) Solutions of the metallaaromatic polymer (**12**) before (left) and after (right) NIR irradiation. Adapted with permission from ref 37. Copyright 2018 Royal Society of Chemistry.

Encouraged by the good photothermal conversion performance of 12C carbolong complexes,[3] we envisage that 12C carbolong complexes could be designed with the core pattern of photothermally responsive materials. Thus, we prepared a cylindrical metallaaromatic polymer with a corn-like nanostructure in which the thermosensitive polymer poly(*N*-isopropylacrylamide) (PNIPAM) links the *α*-cyclodextrin (*α*-CD) cores and the carbolong complex (**13**) (Figure 8).[24] An aqueous solution of the metallaaromatic polymer (**14**) exhibited good NIR-responsive performance due to the grafted metallaaromatic units and induced a phase transition benefiting the thermosensitive PNIPAM units. Polymers **12** and **14** represent new NIR-responsive metallaaromatic polymers and have the potential for NIR laser-triggered drug delivery and controlled release.

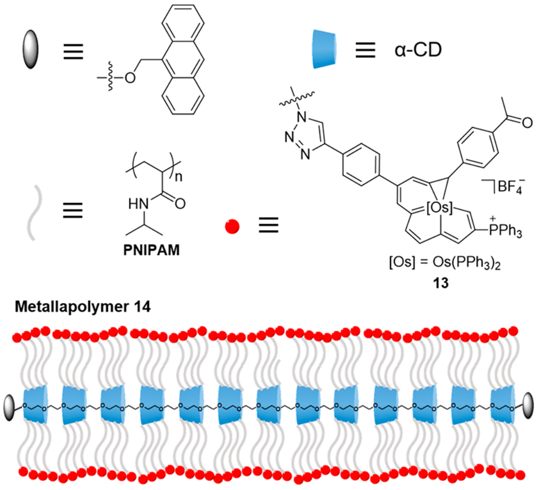

Figure 8. NIR-responsive cylindrical metallaaromatic polymer (**14**). Adapted with permission from ref 24. Copyright 2018 American Chemical Society.

3.2.2. Applications in Photothermally Responsive Self-Healing Materials.

Intrigued by photothermal metallaaromatic polymers in which a phase transition is observed upon exposure to NIR light, we extended the application of 12C carbolong complexes to self-healing materials which possess the ability to autonomously repair damage. To attain this objective, carbolong polyurethanes (CLPUs) were prepared by incorporating a 12C carbolong derivative (**15**) into the backbones of polyurethanes (Figure 9a).[25] The cumulative heat, produced by the incorporated carbolong complex (**15**) under NIR irradiation, resulted in a regional temperature increase. As a result, hydrogen bonding dissociated and the chain diffusion accelerated across the crack, melting polycaprolactone (PCL) crystallites and releasing constraints, promoting the closure of the damaged interfaces. When the light was off, the sample returned to room temperature in association with recrystallization of the PCL segments and reformation of physical interactions. Hence, the sample regained its mechanical properties (Figure 9b). CLPUs exhibited fast photothermal responses and repeatable healing with a high healing efficiency under NIR irradiation (Figure 9c,d).

Motivated by the realization of self-healing CLPUs employing noncovalent interactions such as polymer crystallization and hydrogen bonding, we extended our research to a dynamic polyurethane network (DPUN-1). We introduced a dynamic

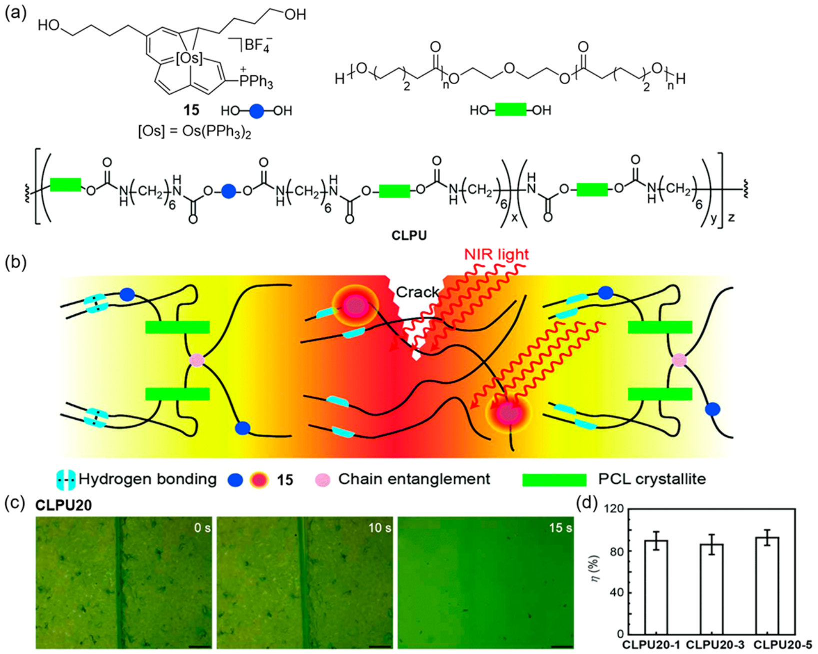

Figure 9. (a) Structure of the 12C carbolong complex (**15**) and the corresponding carbolong polyurethanes (CLPU). (b) Schematic illustration of the NIR-triggered healing process. (c) Optical images of the healing process for CLPU20 (0.20 wt % carbolong complex in polyurethane, scale bar 200 μm) after NIR irradiation. (d) Healing efficiency after multiple notching–healing cycles (1, 3, and 5). Adapted with permission from ref 25. Copyright 2019 Royal Society of Chemistry.

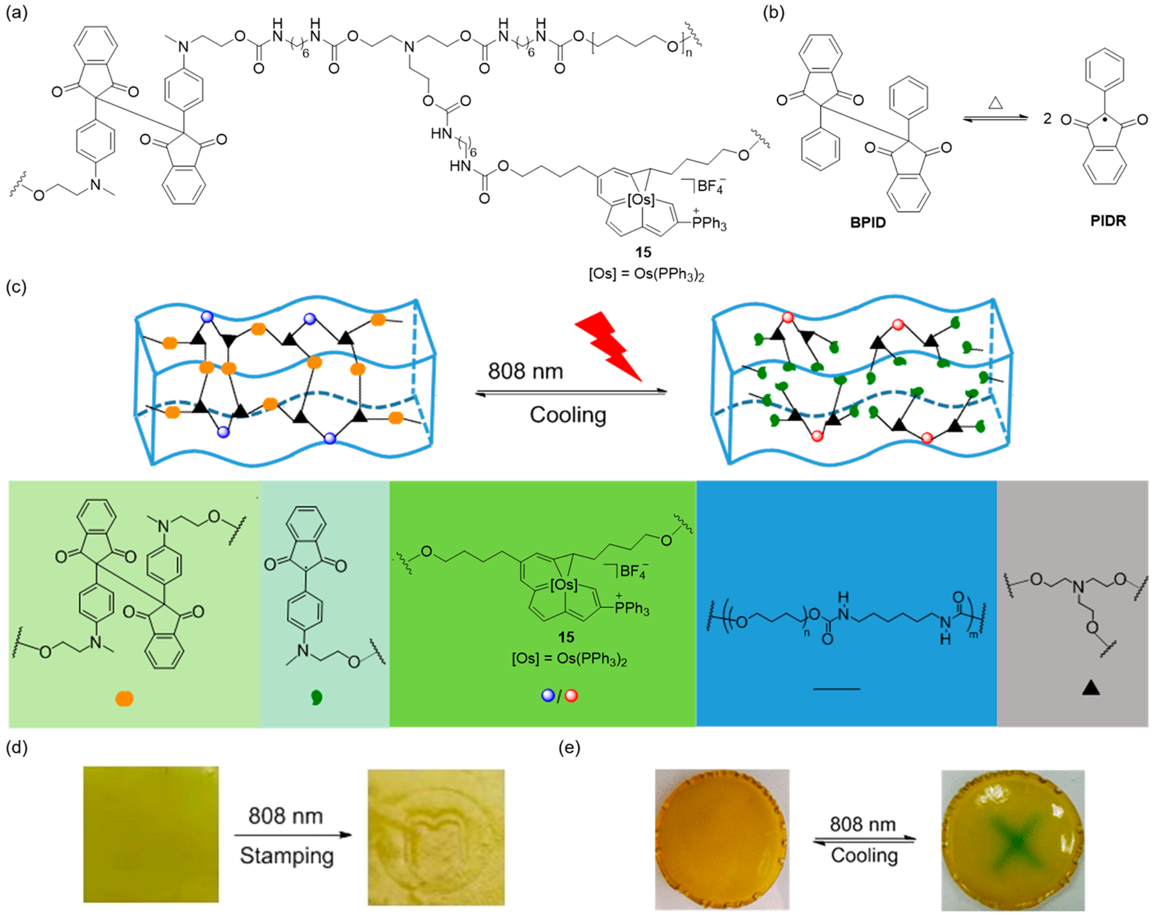

Figure 10. (a) Schematic structures of DPUN-1. (b) Transformation of BPID and PIDR. (c) Schematic illustration of the property of DPUN-1 triggered by NIR light. (d) Pattern stamped onto the surface of the DPUN-1 specimen. (e) rewritable X pattern on the DPUN-1 sheet. Adapted with permission from ref 2. Copyright 2020 American Chemical Society.

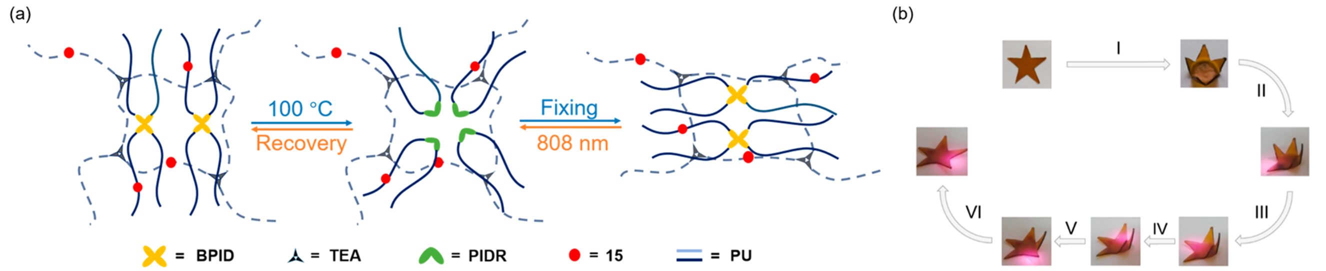

Figure 11. (a) Schematic illustration of the NIR-responsive shape memory of DPUN-2 (TEA represents triethanolamine, a cross-linker in the system). (b) Photographs of shape memory behavior of DPUN-2 by NIR. Adapted with permission from ref 26. Copyright 2021 Elsevier.

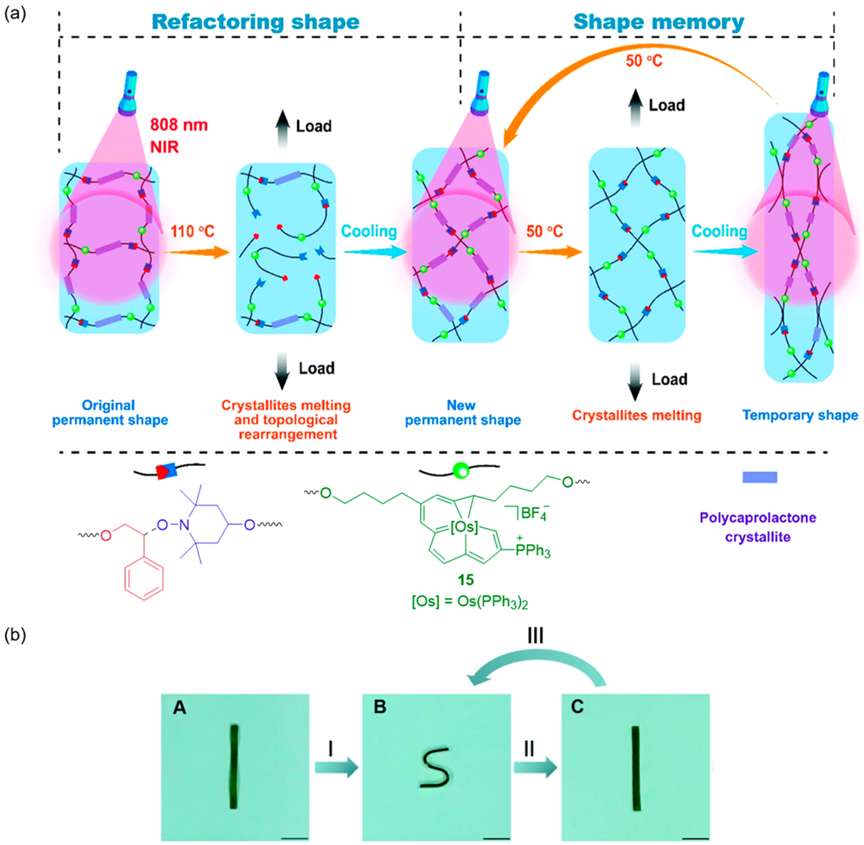

Figure 12. (a) Schematic illustration of the shape memory of the polymer network including TEMPO-based alkoxyamine units. (b) Plastic shape memory of the polymer. Adapted with permission from ref 27. Copyright 2022 Royal Society of Chemistry.

covalent moiety, 2,2′-bis(2-phenylindan-l,3-dione) (BPID), which can undergo thermal homolytic bond dissociation to afford two 2-phenylindan-l,3-dione-yl radicals (PIDR) and a photothermally responsive carbolong complex **15** (Figure 10a,b).[2] Under NIR irradiation, the carbolong moieties generated heat, producing PIDR and reshuffling the segments (Figure 10c). The pattern (the alphabetical M) can be stamped onto the surface of the DPUN specimen under irradiation and remained after removing the light source (Figure 10d). Taking advantage of the thermochromism of the BPID, the DPUN-1 exhibited NIR rewritability. The "X"-shaped pattern created by NIR irradiation through a photomask can be "erased" when the DPUN-1 sheet is cooled to room temperature (Figure 10e).

3.2.3. Applications in Photothermally Responsive Shape Memory Polymers.

Shape memory polymers (SMP), an emerging class of smart materials, are capable of switching between a permanent shape and a temporary shape. They have broad applications in the biomedical field, aerospace engineering, and smart textiles.[38]

The success of self-healing polymers stimulated us to construct a DPUN-based SMP (DPUN-2).[26] The working mechanism is that a temporary shape is initially formed by heating. When the temporary shape was heated by thermal energy that carbolong complex **15** produced under NIR light, the dynamic points were broken once more due to the disassociation of dynamic covalent bonds of BPID, driving the recovery of its initial shape (Figure 11a). To prove the concept, we made a pentagon star-shaped template which was first directly heated and then cooled (Figure 11b). A temporary shape was obtained with each corner folded (step I). Interestingly, the folded sample returned to the flattened shape after the irradiation of each corner, indicating an effective cooperation of carbolong complex's NIR photothermal conversion and BPID's dynamic nature (steps II to VI).

Besides the exploitation of the self-healing and shape memory behaviors of DPUNs containing BPID moieties, we incorporated TEMPO-based alkoxyamine units into the complex dynamic system, thus combining thermally responsive PCL and photothermally responsive carbolong complexes (Figure 12).[27] Compared to DPUN systems, we employed TEMPO-based alkoxyamine as an exchangeable radical unit instead of the BPID, which is tolerant to many functional groups and responds to NIR-mediated permanent shape resetting rather than the remote control of a temporary shape recovery (Figure 12a). Herein, we give an example of resetting a material's permanent shape. First, the temperature of the sample ("I" shape) increased under irradiation, dissociating the dynamic bonds. Subsequently, the removal of irradiation led to the reformation of the dynamic bonds, and the sample was adapted into the new permanent "S" shape because of its plastic property (step I, A → B). Then, upon reheating this sample by NIR irradiation to a relatively low temperature which minimized the dissociation of dynamic bonds, a temporary I shape was realized through the melting and crystallization of PCL segments (step II, B → C). When the sample was reirradiated, the temporary I shape returned to the permanent S shape, thus completing a shape memory cycle (step III, C → B) (Figure 12b).

3.3. Biomedical Applications

Half-sandwich osmium arene complexes with their cytotoxic activity have been proven to be potent anticancer reagents.[39] In contrast, some osmium carbolong complexes exhibit low cell cytotoxicity and good biocompatibility. When combined with the broad absorption in the NIR and good photothermal performance, they produce potential photoacoustic (PA) imaging and photothermal reagents that can be used in cancer treatment. Photodynamic therapy (PDT) applications of a carbolong peroxo complex have also been discovered.

3.3.1. Photothermal Effects and PA Imaging of 9C Carbolong Complexes. 9C carbolong complexes (**16** and **17**) have wide absorption spectra ranging from visible light to NIR. The absorption maxima of **16** and **17** (Figure 13a) in low-energy absorption bands are 672 and 660 nm, respectively (Figure 13b).[21] The photothermal effects of **16** and **17** were further examined under NIR laser irradiation (λ = 808 nm, 1 W cm^{-2}) (Figure 13c). Upon irradiation, a solution of **16** and **17** exhibited a significant temperature increase within 5 min (Figure 13d). A PA imaging study of **16** and **17** showed that the signal intensity significantly rose with the increasing concentrations of substrates (Figure 13e,f). Unfortunately, the biocompatibility of **16** and **17** needs to be improved for further applications *in vivo*. Despite this, they represent the first examples of the photothermal and PA study of metallaromatics and shed light on promising theragnostic agents for PA imaging-guided photothermal cancer therapy.

3.3.2. Photothermal Properties and Phototherapeutic Applications of 12C Carbolong Complexes. Even though 9C carbolong complexes have wide absorption spectra, their NIR absorption is weak and their biocompatibility is poor, both of which impede the phototherapeutic applications *in vivo*. A breakthrough in the applications of carbolong complexes in the biomedical area occurred shortly after a primary photothermal study of 12C carbolong complexes. The absorption maxima of **18** are far more red-shifted compared to those from the 9C carbolong complexes as a consequence of larger π conjugation (Figure 14). As a result, **18** showed more outstanding photothermal effects than **16** and **17**.[3]

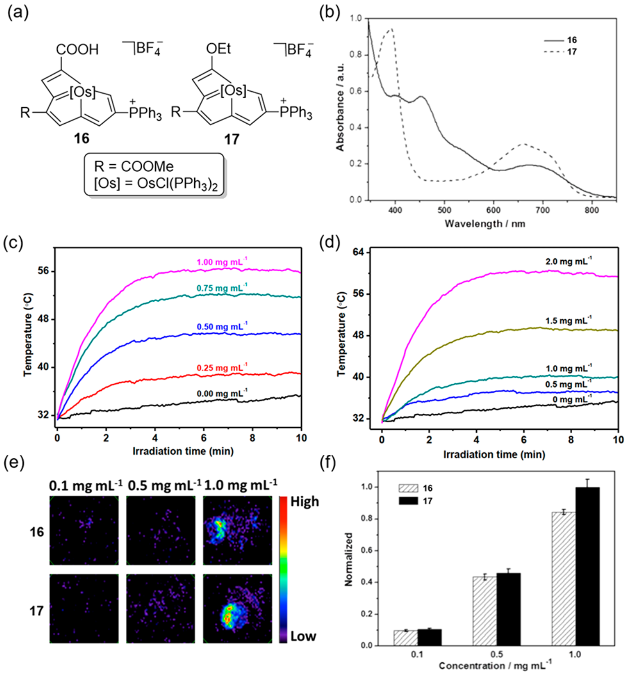

Figure 13. (a) Chemical structures of **16** and **17**. (b) Absorption spectra of **16** and **17**. (c) Photothermal effect of **16**. (d) Photothermal effect of **17**. (e) PA imaging of **16** and **17**. (f) Normalized PA intensity of **16** and **17**. Adapted with permission from ref 21. Copyright 2015 Wiley-VCH Verlag GmbH.

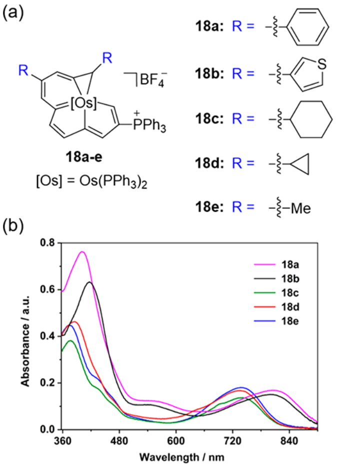

Figure 14. Chemical structures of 12C carbon complexes (**18**) and their absorption spectra. Reproduced with permission from ref 3. Copyright The Authors, some rights reserved; exclusive license American Association for the Advancement of Science. Distributed under a Creative Commons Attribution License 4.0 (CC BY) https://creativecommons.org/licenses/by/4.0/.

To improve the biocompatibility of **18**, **18a@NPs** were prepared by combining the amphiphilic polymer with complex **18a**. To confirm the cytotoxicity of the **18a@NPs**, 3-(4,5-dimethylthiazol-2-yl)-2,5-diphenyltetrazolium bromide (MTT) assays were conducted on SCC7, SCG79011, and 4T1 cell lines following incubation with **18a@NPs**. The cytotoxicity tests show that **18a@NPs** exhibit low cell cytotoxicity and good biocompatibility as evidenced by the high cell viability and good performance of tumor accumulation (Figure 15).

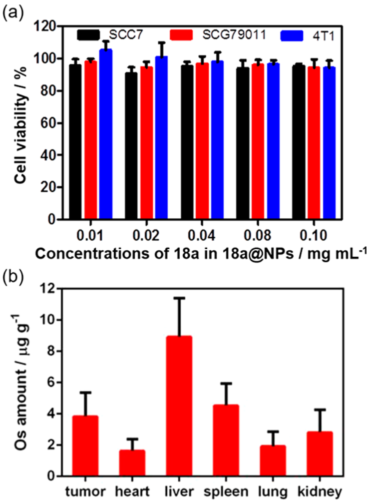

Figure 15. (a) Cytotoxicity of **18a@NPs** measured *in vitro* without laser irradiation. (b) Accumulation of **18a@NPs** in the tumor tissue and clearance organs. Reproduced with permission from ref 3. Copyright The Authors, some rights reserved; exclusive license American Association for the Advancement of Science. Distributed under a Creative Commons Attribution License 4.0 (CC BY) https://creativecommons.org/licenses/by/4.0/.

Photothermal therapy (PTT) is one of the therapy methods that converts light energy (usually NIR light) into heat energy to cause cellular necrosis or apoptosis. Based on comprehensive research on the photothermal performance and biocompatibility of **18a@NPs**, we further utilized **18a@NPs** for PTT treatment of tumors *in vivo*. Under laser irradiation, **18a@NPs** displayed lower SCC7 cell viability than control tests in the absence of laser light (Figure 16a). The tumor in the control experiment grew exponentially with volume, becoming 12 times larger after 14 days (Figure 16b). In contrast, the mice receiving intravenous injections of **18a@NPs** showed irradiation-induced tumor ablation in 2 days and exhibited tumor regression in 14 days (Figure 16c). In this work, metallaaromatics were used for PTT for the first time and the treatment exhibited comparable efficiency to that of common photothermal agents such as nanoporphyrins.[8]

3.3.3. Chemical Modification of 12C Carbolong Complexes to Improve Their Biocompatibility.

In addition to the PEG (poly(ethylene glycol)) blending approach to increase the biocompatibility of **18**, we further developed chemical modifications of 12C carbolong complexes with PEGs of different molecular weight through click reactions.[23] This new type of amphipathic macromolecule (**19**) was assembled into micelles in water (Figure 17). The photothermal properties and cytotoxicity of these assemblies cored with 12C carbolong complexes were essentially the same as those found in **18a@NPs**, indicating that PEG-modified carbolong complexes could serve as promising photothermal theranostic agents.

3.3.4. PA Imaging and PDT Applications of 12C Carbolong Complexes.

At the same time, we prepared MA/SPIOs@AlkylPEI2k-PEG nanoparticles (MASA) from the carbolong complex (**18a**) (MA) and superparamagnetic iron oxide nanoparticle clusters (SPIOs) loaded with a micellar carrier (Alkyl-PEI2k-PEG).[22] MASAs not only have good photothermal conversion efficiency but also produce a potential photodynamic reactive oxygen species (ROS). It is well known that ROS, such as the superoxide anion ($O_2^{\bullet -}$), hydroxyl radical (OH•), and singlet oxygen ($^1O_2$), are highly reactive molecules and have been identified as the main oxidants in cancer treatment. Photothermal and photodynamic therapy achieved a synergistic antitumor effect with the aid of magnetic resonance imaging (MRI) and PA imaging, thus considerably improving the therapeutic efficacy (Figure 18).

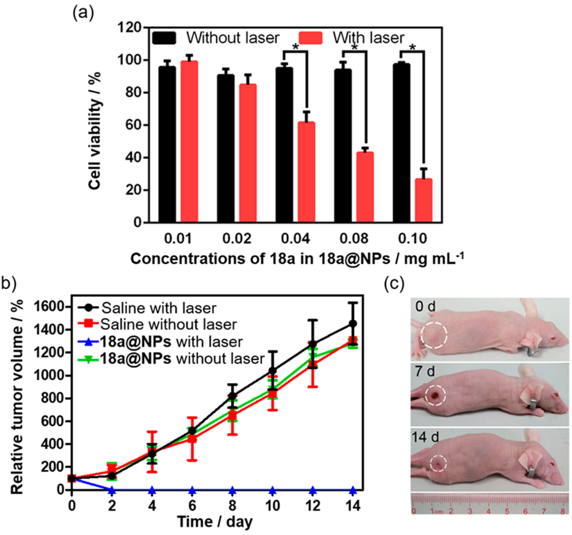

Figure 16. (a) Cell viability of SCC7 cells upon exposure to **18a@NPs** without or with laser irradiation. (b) Tumor growth curves after PTT treatment. (c) Photographs of the SCC7-bearing mice on different days after PTT treatment with **18a@NPs** (laser intensity: λ = 808 nm, 1 W cm^{-2}). Reproduced with permission from ref 3. Copyright The Authors, some rights reserved; exclusive license American Association for the Advancement of Science. Distributed under a Creative Commons Attribution License 4.0 (CC BY) https://creativecommons.org/licenses/by/4.0/.

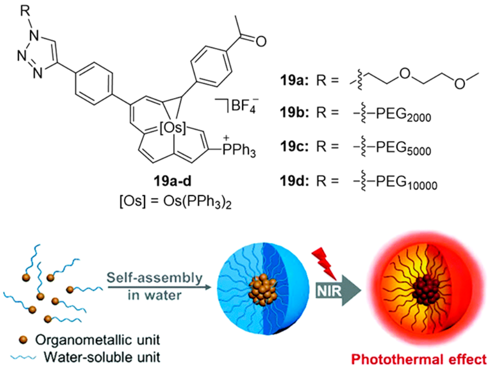

Figure 17. Carbolong complexes containing macromolecules (**19**) and assembled micelles with photothermal properties. Adapted with permission from ref 23. Copyright 2017 Royal Society of Chemistry.

3.3.5. PA Performance and Sonodynamic Effects of 7C Carbolong Complexes Fused with Pyridine 20 and 21.

The properties of metallaaromatics containing heteroatoms have also been investigated. For example, the effective low-energy absorption of complexes **20** and **21** motivated us to study PA imaging properties (Figure 19a,b).[40] The complex (**21**) exhibited a stronger PA signal than complex **20** due to its higher absorption (Figure 19c). Besides PA imaging studies,

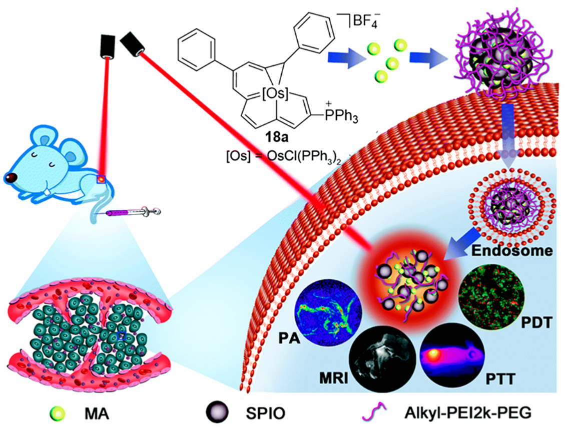

Figure 18. Schematic of MA-loaded nanoparticles for dual-modal MRI/PA imaging-guided synergistic PTT/PDT cancer therapy. Adapted with permission from ref 22. Copyright 2018 Royal Society of Chemistry.

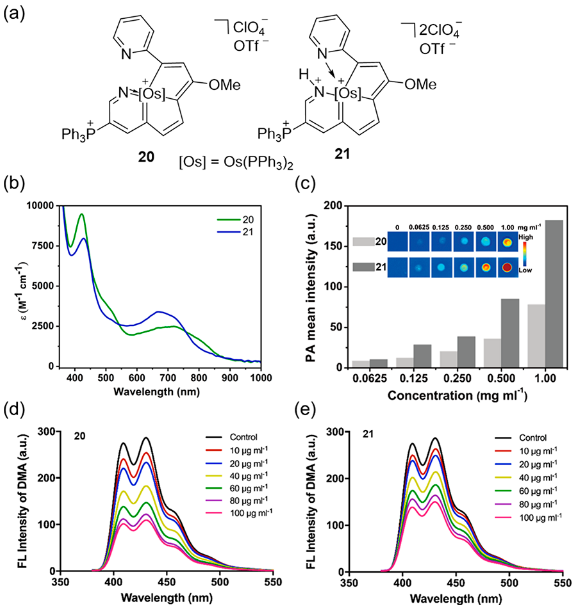

Figure 19. (a) Chemical structures of **20** and **21**. (b) Absorption spectra of **20** and **21**. (c) PA mean intensities of **20** and **21** (inset: PA imaging). (d, e) Assessment of the generation of ROS by **20** and **21** activated by ultrasound. Reproduced with permission from ref 40. Copyright The Authors, some rights reserved; exclusive license Springer Nature. Distributed under a Creative Commons Attribution License 4.0 (CC BY) https://creativecommons.org/licenses/by/4.0/.

we also examined the sonodynamic effects of these compounds. Sonodynamic therapy (SDT), an alternative approach to the treatment of cancer and other diseases, utilizes ultrasound to produce ROS by activating sonosensitizers. This has many benefits such as a greater penetration depth and reduced side effects. The fluorescence intensity of 9,10-dimethylanthracene (DMA, a singlet oxygen detector) decreased as the concentration of **20** and **21** increased, indicating that ROS can be generated with ultrasound (Figure 19d,e). Combined with their good performance of PA imaging, compounds **20** and **21** can be viewed as potential theranostic agents for PA imaging-guided SDT.

3.3.6. Photothermal Properties of 7C Carbolong Complexes with Fused Quinolines (22). Later, we prepared 7C carbolong complexes with fused quinolines (**22**), which have a larger π conjugation compared to that of **20** and **21**. As a result, the absorption extends to the NIR-II for the first time. Moreover, they exhibit good photothermal performance under 1060 nm laser irradiation and can be employed as potent NIR-II photothermal reagents (Figures 20).[41]

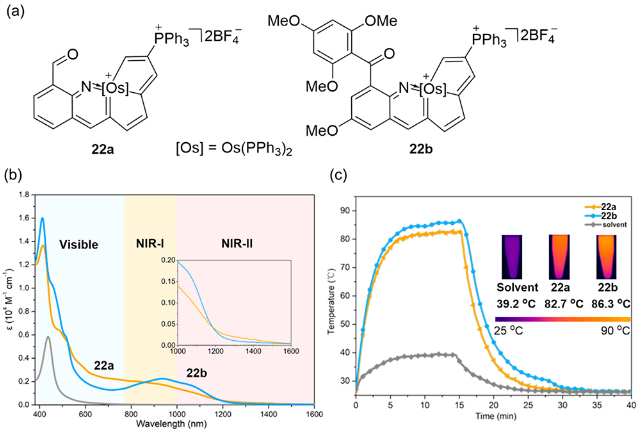

Figure 20. (a) Chemical structures of **22**. (b) Absorption spectra of **22**. (c) Photothermal effect of **22** under 1060 nm. Adapted with permission from ref 41. Copyright 2022 Wiley-VCH Verlag GmbH.

3.3.7. PDT of a Carbolong Peroxo in Hypoxia. On the pathway to applications of ROS produced by carbolong complexes, we learned that PDT usually employs ROS generated exogenously from photosensitizers by light activation. PDT, however, displays a low efficiency under hypoxia resulting from its consumption of limited oxygen present. In this regard, photoactive compounds for the photocontrolled generation of endogenous ROS present significant application possibilities for the treatment of hypoxic tumors. To address this issue, we surmised that a carbolong complex (**23**) with coordinated dioxygen could be employed as an “oxygen shuttle” to facilitate *in situ* oxygen generation. We discovered that the carbolong complex (**23**) was inactive in the dark but under light irradiation led to the release of a superoxide anion $O_2^{\bullet -}$ along with the formation of the cytotoxic osmium complex (**24**) in the absence of oxygen (Figure 21a). Confocal imaging showed that **23** could produce ROS, which induced photocatalytic oxidation reactions of 1,4-dihydronicotinamide adenine dinucleotide in HeLa cells under both normoxia and hypoxia (Figure 21b). *In vivo* studies revealed that the tumor size in the irradiated group treated with **23** was the smallest, effectively inhibiting tumor growth in mice (Figure 21c).[28]

4. APPLICATIONS IN CATALYTIC REACTIONS

Most metallaaromatics can be regarded as carbon-coordinated transition-metal complexes involving cyclic metal carbene or carbyne units. By virtue of their unique structures, their catalytic activities have recently attracted the attention of synthetic chemists. A creative example reported by Lee, Liu, and co-workers[42] revealed that the ruthenabenzenes displayed robust catalytic activity as precatalysts in olefin metathesis, behaving as an analog of the Grubbs-type catalysts with higher stability. Carbolong complexes can be viewed as carbon-based polydentate transition-metal complexes, thus developing dehydrogenation of alcohols by metal−ligand cooperative

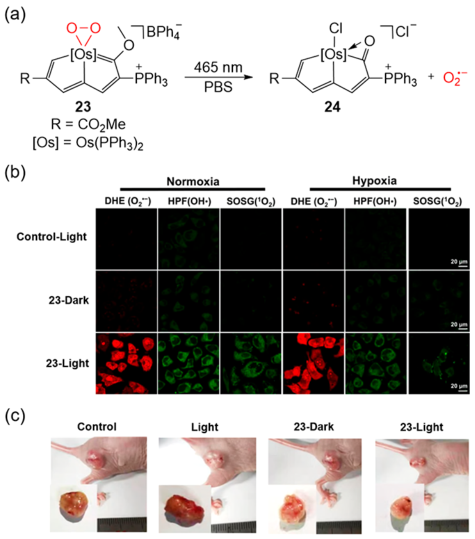

Figure 21. (a) Schematic representation of the release of $O_2^{\bullet-}$, light-mediated by **23**. (b) HeLa cells incubated with **23**. (Dihydroethidium (DHE), hydroxyphenyl fluorescein (HPF), and singlet oxygen sensor green (SOSG) were utilized to probe the production of ROS.) (c) Photographs of representative mice after treatment. Reproduced with permission from ref 28. Copyright The Authors, some rights reserved; exclusive license Springer Nature. Distributed under a Creative Commons Attribution License 4.0 (CC BY) https://creativecommons.org/licenses/by/4.0/.

catalysis through aromatization−dearomatization[29] and the difunctionalization of alkenes by bimetallic cooperative catalysis in a light-induced aerobic process.[4]

4.1. Catalytic Dehydrogenation of Alcohols

We found that the osmium-peroxo (**23**) complex enables the aerobic oxidation of alcohols (Scheme 2).[29] A mechanistic study showed that the reaction proceeded by a concerted double-hydrogen transfer and involved an unusual dearomatization−aromatization process of the CCC pincer complex. This represents the first example of metal−ligand cooperation by aromatization−dearomatization catalysis in a metallaaromatic system.[43,44]

Scheme 2. Aerobic Catalytic Oxidation of Alcohols by 23

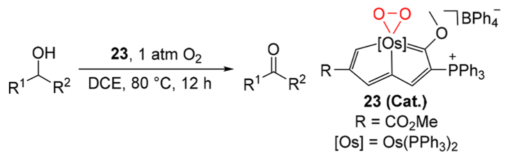

4.2. Cooperative Catalysis by Metal−Metallaaromatics

We also prepared the heterobimetallic CCC pincer molecule (**25**), which is a metal−metallaaromatic complex.[45] In light of the facile chloride ligand substitution at the osmium center, copper-catalyzed difunctionalization of activated alkenes, and the oxygen-stable catalytic performance of the carbolong complex **25**, we found that the carbolong complex **25** via a metal−metallaaromatic synergistic strategy could catalytically difunctionalize unactivated aliphatic alkenes robustly with diphenyl diselenide in combination with a diverse nucleophile such as water, amine, or acid under an oxygen atmosphere at room temperature. This significantly enhances the selectivity, reactivity, and limited substrate scope and encourages us to design other metallaaromatic catalysts and explore more complicated catalytic reactions such as asymmetric catalysis (Scheme 3).[4]

Scheme 3. Schematic Catalytic Reactions by Catalyst 25

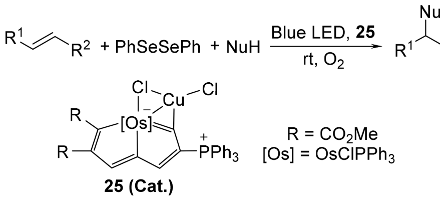

5. OTHER STUDIES OF PROPERTIES AND APPLICATIONS OF METALLAAROMATICS

Some properties and applications are not demonstrated in detail here, but they also show quite promising results, including the theoretical predication for applications of osmapentalynes in third-order nonlinear optical materials,[46−48] photothermal properties of metal-bridged osmaindenes,[49] reversible oxidation of metallapentalenoxazetes,[50] mitochondrial dysfunction by phosphonium-containing metallafurans,[51] NIR-responsive hydrogels containing 12C carbolongs,[52] light-mediated CO_2-responsive metallaaromatic microgels,[53] and hypersaline water treatment.[54] Moreover, we have most recently prepared polycarbolong conjugated polymers that employed metallaaromatics as building blocks, exhibiting optimistic applications in conductive polymers.[55]

6. CONCLUSIONS AND OUTLOOK

As illustrated in this Account, metallaaromatics such as special $d_\pi-p_\pi$ conjugation aromatics can transmit electrons and thus can be employed in single-molecule conductors and ETLs in photovoltaics. Moreover, some have strong, broad absorptions and can convert light energy to light, heat, and ultrasound. As a result, photothermally responsive smart materials and phototherapy reagents with metallaaromatic cores have been developed. Finally, the discovery of catalytic activities based on the CCC pincer transition-metal complexes has been described. These applications deal with some critical issues in energy storage, drug delivery, cancer therapy, and synthetic methodology. The outlined relationship among structures, properties, and applications of aromatic carbolongs could provide pathways to further develop the properties and applications of other metallaaromatics.

Looking ahead, some further explorations of properties and applications of metallaaromatics are viewed as very challenging but intriguing. First, it is essential to pay more attention to theoretical studies on discovering the properties of metallaaromatics. Second, more functional metallaaromatic compounds are the targets of design and development efforts. For example, metallaaromatic radicals and magnetic metallaaromatics, whose aromaticity is the subject of some debate but also which forecast future applications on magnetic materials, and NIR-II materials with metallaaromatic cores could be realized by extending the π-conjugation system. Third, the metallaaromatics could also be employed as alternatives in active layers in solar cells where they could take advantage of their broad absorption. Finally, more catalytic reactions based on metallaaromatics with cyclic metal carbenes or carbynes such as asymmetric catalysis, electrocatalysis, alkyne metathesis, visible light, and even NIR photocatalysis may be discovered.

AUTHOR INFORMATION

Corresponding Author

Haiping Xia − *Shenzhen Grubbs Institute, Department of Chemistry, Southern University of Science and Technology, Shenzhen 518055, China; State Key Laboratory of Physical Chemistry of Solid Surfaces, College of Chemistry and Chemical Engineering, Xiamen University, Xiamen 361005, China;* orcid.org/0000-0002-2688-6634; Email: xiahp@sustech.edu.cn

Authors

Ming Luo − *Shenzhen Grubbs Institute, Department of Chemistry, Southern University of Science and Technology, Shenzhen 518055, China*

Dafa Chen − *Shenzhen Grubbs Institute, Department of Chemistry, Southern University of Science and Technology, Shenzhen 518055, China;* orcid.org/0000-0002-7650-4024

Qian Li − *State Key Laboratory of Physical Chemistry of Solid Surfaces, College of Chemistry and Chemical Engineering, Xiamen University, Xiamen 361005, China*

Complete contact information is available at: https://pubs.acs.org/10.1021/acs.accounts.2c00750

Author Contributions

CRediT: **Ming Luo** conceptualization (equal), methodology (equal), writing-original draft (lead), writing-review & editing (lead); **Dafa Chen** data curation (lead), formal analysis (equal), investigation (supporting); **Qian Li** resources (equal), validation (equal), visualization (equal); **Haiping Xia** conceptualization (lead), funding acquisition (lead), project administration (lead), supervision (lead), writing-review & editing (lead).

Notes

The authors declare no competing financial interest.

Biographies

Ming Luo obtained his Ph.D. in chemistry from Xiamen University in 2016 under the supervision of Prof. Haiping Xia. Then he worked with Prof. H. Zhao at UESTC and A. Herrmann at DWI-RWTH as a postdoctoral fellow. In 2020, he returned to the Xia group. His research focuses on the properties and applications of carbolong complexes.

Dafa Chen earned his Ph.D. in chemistry from Nankai University in 2008, advised by Shansheng Xu. From 2008 to 2011, he worked as a postdoctoral fellow at École Polytechnique Fédérale de Lausanne (EPFL) After that, he joined Harbin Institute of Technology as a full professor. In 2020, he started to work at Southern University of Science and Technology, and his current research interests include catalysis and small-molecule activation.

Qian Li received her B.S. degree in 2017 from Xiamen University and continued studying for her Ph.D. at the same institution under the supervision of Prof. Haiping Xia. She is working on the synthesis and reactivity of metallacycles.

Haiping Xia received his B.S. and M.S. degrees from Xiamen University in 1983 and 1986, respectively. Following that, he continued to work at the same university, and from 1995 to 1997, he went to Hong Kong University of Science and Technology as a visiting scholar. Two years later, he was appointed a full professor at Xiamen University. In 2018, he joined Southern University of Science and Technology as the Chair Professor. He received the Huang Yao-Zeng Organometallic Chemistry Award and the National Natural Science Award of China. His group's research interests are focused on carbolong chemistry.

ACKNOWLEDGMENTS

We thank all of our co-workers for their innovative work on this topic. M.L. thanks Xinjia Cai and Yuhui Hua for drafting the table of contents graphic. We gratefully acknowledge the Natural Science Foundation of China (nos. 21931002, 22071098, 92156021, and 22101115), the Shenzhen Science and Technology Innovation Committee (nos. JCYJ20200109140812302 and JCYJ20210324105013035), and the Guangdong Provincial Key Laboratory of Catalysis (no. 2020B121201002). We are also grateful for financial support from the Outstanding Talents Training Fund in Shenzhen.

REFERENCES

(1) Liu, L.; Chen, S.; Qu, Y.; Gao, X.; Han, L.; Lin, Z.; Yang, L.; Wang, W.; Zheng, N.; Liang, Y.; Tan, Y.; Xia, H.; He, F. Nanographene-Osmapentalyne Complexes as a Cathode Interlayer in Organic Solar Cells Enhance Efficiency over 18%. *Adv. Mater.* **2021**, *33*, 2101279.

(2) Chen, Y.; Yang, L.; Zheng, W.; Ouyang, P.; Zhang, H.; Ruan, Y.; Weng, W.; He, X.; Xia, H. Dynamic Polymer Network System Mediated by Radically Exchangeable Covalent Bond and Carbolong Complex. *ACS Macro Lett.* **2020**, *9*, 344−349.

(3) Zhu, C.; Yang, C.; Wang, Y.; Lin, G.; Yang, Y.; Wang, X.; Zhu, J.; Chen, X.; Lu, X.; Liu, G.; Xia, H. CCCCC Pentadentate Chelates with Planar Möbius Aromaticity and Unique Properties. *Sci. Adv.* **2016**, *2*, e1601031.

(4) Cui, F.-H.; Hua, Y.; Lin, Y.-M.; Fei, J.; Gao, L.-H.; Zhao, X.; Xia, H. Selective Difunctionalization of Unactivated Aliphatic Alkenes Enabled by a Metal-Metallaaromatic Catalytic System. *J. Am. Chem. Soc.* **2022**, *144*, 2301−2310.

(5) Fernandez, I. *Aromaticity: Modern Computational Methods and Applications*; Elsevier: 2021.

(6) Mortier, J. *Arene Chemistry: Reaction Mechanisms and Methods for Aromatic Compounds*; John Wiley & Sons: 2016.

(7) Huang, J.; Yu, G. Structural Engineering in Polymer Semiconductors with Aromatic N-Heterocycles. *Chem. Mater.* **2021**, *33*, 1513−1539.

(8) Faustova, M.; Nikolskaya, E.; Sokol, M.; Fomicheva, M.; Petrov, R.; Yabbarov, N. Metalloporphyrins in Medicine: From History to Recent Trends. *ACS Appl. Bio Mater.* **2020**, *3*, 8146−8171.

(9) Elliott, G. P.; Roper, W. R.; Waters, J. M. Metallacyclohexatrienes or 'Metallabenzenes.' Synthesis of Osmabenzene Derivatives and X-ray Crystal Structure of [Os(CSCHCHCHCH)(CO)(PPh_3)$_2$]. *J. Chem. Soc., Chem. Commun.* **1982**, 811−813.

(10) Thorn, D. L.; Hoffmann, R. Delocalization in Metallocycles. *Nouv. J. Chim.* **1979**, *3*, 39−45.

(11) Chen, D.; Hua, Y.; Xia, H. Metallaaromatic Chemistry: History and Development. *Chem. Rev.* **2020**, *120*, 12994−13086.

(12) Zhu, C.; Xia, H. Carbolong Chemistry: A Story of Carbon Chain Ligands and Transition Metals. *Acc. Chem. Res.* **2018**, *51*, 1691−1700.

(13) Frogley, B. J.; Wright, L. J. Recent Advances in Metallaaromatic Chemistry. *Chem. - Eur. J.* **2018**, *24*, 2025−2038.

(14) Wright, L. J. *Metallabenzenes: An Expert View*; John Wiley & Sons Ltd: Hoboken, NJ, 2017.

(15) Chen, J.; Jia, G. Recent Development in the Chemistry of Transition Metal-containing Metallabenzenes and Metallabenzynes. *Coord. Chem. Rev.* **2013**, *257*, 2491−2521.

(16) Wei, J.; Zhang, W.-X.; Xi, Z. The Aromatic Dianion Metalloles. *Chem. Sci.* **2018**, *9*, 560−568.

(17) Zhang, Y.; Yu, C.; Huang, Z.; Zhang, W.-X.; Ye, S.; Wei, J.; Xi, Z. Metalla-aromatics: Planar, Nonplanar, and Spiro. *Acc. Chem. Res.* **2021**, *54*, 2323−2333.

(18) Wang, H.; Zhou, X.; Xia, H. Metallaaromatics Containing Main-group Heteroatoms. *Chin. J. Chem.* **2018**, *36*, 93−105.

(19) Zhu, C.; Luo, M.; Zhu, Q.; Zhu, J.; Schleyer, P. v. R.; Wu, J. I.-C.; Lu, X.; Xia, H. Planar Möbius Aromatic Pentalenes Incorporating 16 and 18 Valence Electron Osmiums. *Nat. Commun.* **2014**, *5*, 3265.

(20) Zhu, C.; Li, S.; Luo, M.; Zhou, X.; Niu, Y.; Lin, M.; Zhu, J.; Cao, Z.; Lu, X.; Wen, T.; Xie, Z.; Schleyer, P. v. R.; Xia, H. Stabilization of Anti-Aromatic and Strained Five-Membered Rings with a Transition Metal. *Nat. Chem.* **2013**, *5*, 698−703.

(21) Zhu, C.; Yang, Y.; Luo, M.; Yang, C.; Wu, J.; Chen, L.; Liu, G.; Wen, T.; Zhu, J.; Xia, H. Stabilizing Two Classical Antiaromatic Frameworks: Demonstration of Photoacoustic Imaging and the Photothermal Effect in Metalla-aromatics. *Angew. Chem., Int. Ed.* **2015**, *54*, 6181−6185.

(22) Yang, C.; Lin, G.; Zhu, C.; Pang, X.; Zhang, Y.; Wang, X.; Li, X.; Wang, B.; Xia, H.; Liu, G. Metalla-Aromatic Loaded Magnetic Nanoparticles for MRI/Photoacoustic Imaging-Guided Cancer Phototherapy. *J. Mater. Chem. B* **2018**, *6*, 2528−2535.

(23) He, X.; He, X.; Li, S.; Zhuo, K.; Qin, W.; Dong, S.; Chen, J.; Ren, L.; Liu, G.; Xia, H. Amphipathic Metal-containing Macromolecules with Photothermal Properties. *Polym. Chem.* **2017**, *8*, 3674−3678.

(24) Lu, Z.; Lin, Q.; Cai, Y.; Chen, S.; Chen, J.; Wu, W.; He, X.; Xia, H. Cylindrical NIR-Responsive Metallopolymer Containing Möbius Metalla-Aromatics. *ACS Macro Lett.* **2018**, *7*, 1034−1038.

(25) Zhang, H.; Zhao, H.; Zhuo, K.; Hua, Y.; Chen, J.; He, X.; Weng, W.; Xia, H. "Carbolong" Polymers with Near Infrared Triggered, Spatially Resolved and Rapid Self-Healing Properties. *Polym. Chem.* **2019**, *10*, 386−394.

(26) Yang, L.; Ouyang, P.; Chen, Y.; Xiang, S.; Ruan, Y.; Weng, W.; He, X.; Xia, H. Tough Self-Reporting Elastomer with NIR Induced Shape Memory Effect. *Giant* **2021**, *8*, 100069.

(27) Yang, L.; Zhao, H.; Xie, Y.; Ouyang, P.; Ruan, Y.; Chen, J.; Weng, W.; He, X.; Xia, H. Optically Reconfigurable Shape Memory Metallopolymer Mediated by a Carbolong Complex and Radically Exchangeable Covalent Bond. *Polym. Chem.* **2022**, *13*, 1844−1851.

(28) Lu, N.; Deng, Z.; Gao, J.; Liang, C.; Xia, H.; Zhang, P. An Osmium-peroxo Complex for Photoactive Therapy of Hypoxic Tumors. *Nat. Commun.* **2022**, *13*, 2245.

(29) Deng, Z.; Wu, P.; Cai, Y.; Sui, Y.; Chen, Z.; Zhang, H.; Wang, B.; Xia, H. Dioxygen Activation by Internally Aromatic Metallacycle: Crystallographic Structure and Mechanistic Investigations. *iScience* **2020**, *23*, 101379.

(30) Li, R.; Lu, Z.; Cai, Y.; Jiang, F.; Tang, C.; Chen, Z.; Zheng, J.; Pi, J.; Zhang, R.; Liu, J.; Chen, Z.; Yang, Y.; Shi, J.; Hong, W.; Xia, H. Switching of Charge Transport Pathways via Delocalization Changes in Single-Molecule Metallacycles Junctions. *J. Am. Chem. Soc.* **2017**, *139*, 14344−14347.

(31) Chen, S.; Liu, L.; Gao, X.; Hua, Y.; Peng, L.; Zhang, Y.; Yang, L.; Tan, Y.; He, F.; Xia, H. Addition of Alkynes and Osmium Carbynes towards Functionalized d_π-p_π Conjugated Systems. *Nat. Commun.* **2020**, *11*, 4651.

(32) Wang, J.; Li, J.; Zhou, Y.; Yu, C.; Hua, Y.; Yu, Y.; Li, R.; Lin, X.; Chen, R.; Wu, H.; Xia, H.; Wang, H. L. Tuning an Electrode Work Function Using Organometallic Complexes in Inverted Perovskite Solar Cells. *J. Am. Chem. Soc.* **2021**, *143*, 7759−7768.

(33) Li, J.; Wang, J.; Zhou, Y.; Yu, C.; Liu, H.; Qi, X.; Li, R.; Hua, Y.; Yu, Y.; Chen, R.; Chen, D.; Mao, L.; Xia, H.; Wang, H. L. Boosting the Performance and Stability of Inverted Perovskite Solar Cells by Using a Carbolong Derivative to Modulate the Cathode Interface. *Mater. Chem. Front.* **2022**, *6*, 2211−2218.

(34) Liu, H.; Lu, Z.; Zhang, W.; Wang, J.; Lu, Z.; Dai, Q.; Qi, X.; Shi, Y.; Hua, Y.; Chen, R.; Shi, T.; Xia, H.; Wang, H. L. Anchoring Vertical Dipole to Enable Efficient Charge Extraction for High-Performance Perovskite Solar Cells. *Adv. Sci.* **2022**, *9*, 2203640.

(35) Moore, E. G.; Samuel, A. P. S.; Raymond, K. N. From Antenna to Assay: Lessons Learned in Lanthanide Luminescence. *Acc. Chem. Res.* **2009**, *42*, 542−552.

(36) Bahl, S.; Nagar, H.; Singh, I.; Sehgal, S. Smart Materials Types, Properties and Applications: A Review. *Mater. Today Proc.* **2020**, *28*, 1302−1306.

(37) Lu, Z.; Cai, Y.; Wei, Y.; Lin, Q.; Chen, J.; He, X.; Li, S.; Wu, W.; Xia, H. Photothermal Möbius Aromatic Metallapentalenofuran and Its NIR-Responsive Copolymer. *Polym. Chem.* **2018**, *9*, 2092−2100.

(38) Xia, Y.; He, Y.; Zhang, F.; Liu, Y.; Leng, J. A Review of Shape Memory Polymers and Composites: Mechanisms, Materials, and Applications. *Adv. Mater.* **2021**, *33*, 2000713.

(39) Meier-Menches, S. M.; Gerner, C.; Berger, W.; Hartinger, C. G.; Keppler, B. K. Structure-activity Relationships for Ruthenium and Osmium Anticancer Agents-towards Clinical Development. *Chem. Soc. Rev.* **2018**, *47*, 909−928.

(40) Zhou, X.; Pang, X.; Nie, L.; Zhu, C.; Zhuo, K.; Zhuo, Q.; Chen, Z.; Liu, G.; Zhang, H.; Lin, Z.; Xia, H. Successive Modification of Polydentate Complexes Gives Access to Planar Carbon- and Nitrogen-based Ligands. *Nat. Commun.* **2019**, *10*, 1488.

(41) Cui, F.-H.; Li, Q.; Gao, L.-H.; Ruan, K.; Ma, K.; Chen, S.; Lu, Z.; Fei, J.; Lin, Y.-M.; Xia, H. Condensed Osmaquinolines with NIR-II Absorption Synthesized by Aryl C-H Annulation and Aromatization. *Angew. Chem., Int. Ed.* **2022**, *61*, e202211734.

(42) Gupta, S.; Su, S.; Zhang, Y.; Liu, P.; Wink, D. J.; Lee, D. Ruthenabenzene: A Robust Precatalyst. *J. Am. Chem. Soc.* **2021**, *143*, 7490−7500.

(43) Gunanathan, C.; Milstein, D. Metal-Ligand Cooperation by Aromatization-Dearomatization: A New Paradigm in Bond Activation and "Green" Catalysis. *Acc. Chem. Res.* **2011**, *44*, 588−602.

(44) Gonçalves, T. P.; Dutta, I.; Huang, K.-W. Aromaticity in Catalysis: Metal Ligand Cooperation via Ligand Dearomatization and Rearomatization. *Chem. Commun.* **2021**, *57*, 3070−3082.

(45) Zhou, X.; Li, Y.; Shao, Y.; Hua, Y.; Zhang, H.; Lin, Y.-M.; Xia, H. Reactions of Cyclic Osmacarbyne with Coinage Metal Complexes. *Organometallics* **2018**, *37*, 1788−1794.

(46) Wang, Z.; Yan, W.; Zhao, G.; Wu, K.; Gu, Z.-G.; Li, Q.-H.; Zhang, J. Novel Third-Order Nonlinear Optical Materials with Craig-Möbius Aromaticity. *J. Phys. Chem. Lett.* **2021**, *12*, 11784−11789.

(47) Wang, Z.; Fang, Y.-H.; Lin, H.; Zhao, G.; Yan, W.; Ma, Z.; Li, Q.-H.; Zhang, J. Bucket Effect to Improve Third-Order Nonlinear Optical Response on Metal-Heteroaromatic Compounds. *Chin. J. Chem.* **2022**, *40*, 2611−2617.

(48) Wang, L.; Ye, J.; Wang, H.; Xie, H.; Qiu, Y. The novel link between planar möbius aromatic and third order nonlinear optical properties of metal-bridged polycyclic complexes. *Sci. Rep.* **2017**, *7*, 10182.

(49) Luo, M.; Long, L.; Zhang, H.; Yang, Y.; Hua, Y.; Liu, G.; Lin, Z.; Xia, H. Reactions of Isocyanides with Metal Carbyne Complexes: Isolation and Characterization of Metallacyclopropenimine Intermediates. *J. Am. Chem. Soc.* **2017**, *139*, 1822−1825.

(50) Deng, Z.; Zhu, C.; Hua, Y.; He, G.; Guo, Y.; Lu, R.; Cao, X.; Chen, J.; Xia, H. Synthesis and Characterization of Metallapentalenoxazetes from the [2 + 2] Cycloaddition of Metallapentalynes with Nitrosoarenes. *Chem. Commun.* **2019**, *55*, 6237−6240.

(51) Yeung, C.-F.; Chung, L.-H.; Ng, S.-W.; Shek, H.-L.; Tse, S.-Y.; Chan, S.-C.; Tse, M.-K.; Yiu, S.-M.; Wong, C.-Y. Phosphonium-Ring-Fused Bicyclic Metallafuran Complexes of Ruthenium and Osmium. *Chem.—Eur. J.* **2019**, *25*, 9159−9163.

(52) Lin, X.; Xie, W.; Lin, Q.; Cai, Y.; Hua, Y.; Lin, J.; He, G.; Chen, J. NIR-Responsive Metal-containing Polymer Hydrogel for Light-controlled Microvalve. *Polym. Chem.* **2021**, *12*, 3375−3382.

(53) Wang, X.; Lin, X.; Qiu, H.; Xie, J.; Lu, Z.; Wang, Y.; Wu, W. Light-mediated CO_2-responsiveness of Metallopolymer Microgels. *Chin. Chem. Lett.* **2022**, *33*, 1445−1449.

(54) Wang, M.; He, W.; Hua, Y.; Xie, X.; Chen, S.; Zhou, L.; Zhang, Y.; Hou, Y.; Lin, S.; Xia, H.; Zheng, J.; Hou, X. Alternative Photothermal/electrothermal Hierarchical Membrane for Hypersaline Water Treatment. *SusMat* **2022**, *2*, 679−688.

(55) Chen, S.; Peng, L.; Liu, Y.; Gao, X.; Zhang, Y.; Tang, C.; Zhai, Z.; Yang, L.; Wu, W.; He, X.; Liu, L. L.; He, F.; Xia, H. Conjugated Polymers Based on Metalla-aromatic Building Blocks. *Proc. Natl. Acad. Sci. U. S. A.* **2022**, *119*, No. e2203701119.